Solid-State Reaction between Zinc Hydroxide and 8-Quinolinol

Bharat Lal DUBEY* and Neeta TIWARI
Department of Chemistry, University of Gorakhpur, Gorakhpur, (U.P.), India
(Received May 7, 1991)

Solid-state reaction between zinc hydroxide and 8-quinolinol [8-HQ] has been studied. Reaction product has been characterized to be $Zn(OH)_2(8\text{-}HQ)_2$ by elemental analysis, quantitative estimation of zinc, thermal decomposition in air, thermogravimetry in nitrogen atmosphere, powder X-ray diffraction patterns, and IR spectra. Kinetics of reaction has been investigated by capillary method at different temperatures. Energy of activation for the reaction has been found to be 45.27 kJ mol^{-1}.

Formation of coordination complexes of 8-quinolinol with several metal ions in solution has been studied extensively. It is only recently that solid-state reactions of 8-quinolinol with thallium carbonate,[1] carbonates of zinc and cadmium,[2] and copper(II) acetate[3] have been reported. Solid-state reaction products have been characterized to be $Tl_2CO_3(8\text{-}HQ)_2$, $MCO_3(8\text{-}HQ)_2$ [M= zinc and cadmium], and $Cu(C_9H_6ON)_2$. In these investigations the crystal imperfections have been assumed to facilitate the diffusion of 8-quinolinol leading to the formation of reaction products.

It has been reported that $M(OH)_2$ [M=Mg, Mn, Ca, Fe, Co, Ni, and Cd] have got layered structures similar to that of cadmium iodide. Other hydroxides such as $Cu(OH)_2$, $Zn(OH)_2$, $Al(OH)_3$, and hydroxide oxide of type FeO·OH, CrO·OH, CoO·OH etc. have also got the layered structures.[4] These structures are all built of HO–M–OH layers held together by weak van der Waals' forces and differ only in close packed layer sequences. The weakly bonded layers are flexible and subject to expand on intercalation of certain organic molecules in the interlayer space.[5] It is quite possible that the interlayer space in the crystals of dihydroxides of the metals may facilitate the inner penetration of reacting molecules in the solid state. Based on this presumption it was thought interesting to investigate the solid-state reaction between 8-quinolinol and $M(OH)_2$ [M=Ni, Cu, and Zn]. In this paper we report the investigations on reaction between $Zn(OH)_2$ and 8-quinolinol only. Yellow colored solid-state reaction product has been isolated and characterized. Kinetics of the reaction has been studied by capillary method[6–8] at different temperatures. A probable mechanism for the propagation of reaction has been proposed.

Experimental

Materials Used. Zinc(II) Hydroxide. It was prepared[9] by adding sodium hydroxide (G.R.) to a solution of zinc(II) sulfate (G.R.) [S.M. Chemicals, India]. White precipitate was filtered, washed for the removal of sulfate ions and dried. The purity of zinc(II) hydroxide was checked by quantitative estimation of zinc gravimetrically as ammonium zinc phosphates[10] [Percentage of zinc: found 65.32; calcd for $Zn(OH)_2$ 65.78%] and also by its thermal decomposition to zinc(II) oxide [Percentage of zinc(II) oxide: found 81.56; calcd 81.88%].

8-Quinolinol (8-HQ): It was procured from Aldrich Chemical Company, U.S.A. Its purity was checked by determining the melting point [Found 74.5 °C; reported, 73.5—75.5 °C].

Isolation of Reaction Product: Zinc(II) hydroxide and 8-HQ were mixed in 1:2 molar ratio with 8-HQ in slight excess quantity. The mixture was crushed thoroughly using an agate pestle-mortar and then taken in a tube fitted with standard joint. The tube was closed with stopper fitted with statandard joint and then placed in an incubator at 50±1 °C, for 50 h. The contents of the tube were taken out, crushed, taken in the tube again and placed in the incubator at the same temperature for another 50 h to ensure the completion of reaction. The reaction product so obtained was washed with acetone to remove unreacted 8-HQ and dried. The yellow colored product was characterized.

Characterization of Reaction Product: Elemental Analysis: Carbon, hydrogen, and nitrogen analyses of solid-state reaction product and zinc oxinate prepared from solution[11] was done with the help of an elemental analyzer at Central Drug and Research Institute, (CDRI), Lucknow, (India).

Estimation of Zinc: Zinc content of reaction product was estimated as ammonium zinc phosphate (NH_4ZnPO_4) using standard gravimetric technique.[10]

Thermal Decomposition in Air: For this purpose, weighed amount of reaction product was taken in a cleaned and weighed silica crucible, first heated on low flame of a Bunsen burner and then in an electric furnace at 600 °C for 2 h. The crucible containing the residue was cooled in a desiccator and weighed. The process of heating, cooling, and weighing was repeated till a constant weight was obtained. From the weight of the residue [ZnO] the composition of reaction product was established.

TG Studies: TG curve of solid-state reaction product was obtained from Regional Sophisticated Instrumentation Centre (RSIC), Nagpur, (India) using a Perkin–Elmer thermal analyzer in nitrogen atmosphere from ambient temperature to 930 °C. The heating rate was 10 K min^{-1}.

X-Ray Diffraction Studies: Powder X-ray diffraction patterns of reactants [$Zn(OH)_2$ and 8-HQ], solid-state reaction product, and zinc oxinate prepared from solution[11] were obtained by means of an X-ray diffractometer using Cu$K\alpha$ radiation at RSIC, Nagpur, (India).

IR Spectral Studies: IR spectra of zinc(II) hydroxide, 8-HQ, and solid-state reaction product were taken with the help of a Perkin–Elmer model 881 IR Spectrophotometer at CDRI, Lucknow in nujol mull.

Kinetic Studies: Kinetics of the reaction in solid state was studied by capillary method[6–8] as adopted by earlier workers.

Pyrex glass capillaries (5 cm long, external diameter 8.0 mm, internal diameter 3.0 mm) were used. One end of the capillary was sealed with sealing wax and half the portion was filled with zinc(II) hydroxide (particle size 150—200 mesh sieves) which was dried at 70 °C. The kinetic data may be expected to depend on powder packing in capillaries. However, this did not affect the result as the capillaries were filled by taking successively very small amount of zinc(II) hydroxide followed by gentle tapping on the table for five min each time. The surface of zinc(II) hydroxide in the capillary was smoothened with the help of a thin glass rod by observing under a microscope. The remaining portion of the capillary was cleaned and filled with 8-HQ in contact with zinc(II) hydroxide. The other end of the capillary was also sealed. The capillary containing the reactants in contact was placed in an incubator whose temperature was maintained constant to ±1 °C. The occurrence of the reaction was noted at the interface of the reactants by the formation of yellow colored product. The length of the colored product increased with time. The kinetics was followed by measuring the length of colored product layer at different time intervals with the help of a travelling microscope [least count ±0.001 cm]. The experiments were performed at 40, 50, 60, and 70 °C.

kinetic study was also performed with reactants separated by air-gap of different lengths at 50±1 °C.

In order to understand the effect of particle size on the mode of diffusion of 8-HQ through zinc(II) hydroxide, kinetic studies were performed with reactants of different particle sizes [200—240, 240—300, 300—350 mesh sieves] at 40, 50, 60, and 70 °C.

Results and Discussion

On mixing zinc(II) hydroxide and 8-HQ in 1 : 2 molar ratio, the reaction started with the formation of yellow colored product. Colored product may be either $Zn(OH)_2(8\text{-}HQ)_2$ or $Zn(C_9H_6ON)_2$, a complex formed from solution. Therefore, formation of the colored product in the solid state may take place according to one of the following chemical equations.

(A) $Zn(OH)_2 + 2(8\text{-}HQ) \rightarrow Zn(OH)_2(8\text{-}HQ)_2$
(white) (white) yellow

(B) $Zn(OH)_2 + 2(8\text{-}HQ) \rightarrow Zn(C_9H_6ON)_2 + 2H_2O$
yellow

Data given in Tables 1 and 2 show that the composition of solid-state reaction product is $Zn(OH)_2(8\text{-}HQ)_2$ and not $Zn(C_9H_6ON)_2$ (complex formed in solution). If the composition of reaction product was $Zn(C_9H_6ON)_2$, evolution of H_2O should take place during the course of reaction in solid-state. In order to examine this point a simple experiment was done by using a setup (Fig. 1) made of Corning glass. Anhydrous copper(II) sulfate did not turn blue discarding the evolution of H_2O. Hence, $Zn(C_9H_6ON)_2$ is not the composition of reaction product. TG data (Table 3) derived from TG curve (Fig. 2) also support the composition of reaction product to be $Zn(OH)_2(8\text{-}HQ)_2$. An examination of powder X-ray diffraction patterns (Fig. 3) and interplanar spacing (D) corresponding to main strong lines (Table 4) of reactants, solid-state reaction product, and $Zn(C_9H_6ON)_2$ (prepared from solution) show that the reaction product is certainly a new compound differing from

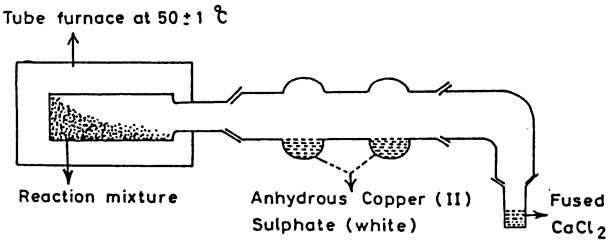

Fig. 1. Experimental set up for testing evolution of H_2O during the reaction.

Table 1. Elemental Analysis Data

Compound	Percentage of elements					
	Found			Calcd		
	C	H	N	C	H	N
$Zn(OH)_2(8\text{-}HQ)_2$	55.20	3.99	7.07	55.48	4.10	7.19
$Zn(C_9H_6ON)_2$[a)]	60.95	3.38	7.80	61.13	3.39	7.92

a) Zinc oxinate prepared from solution.[11)]

Table 2. Data on Thermal Decomposition of Reaction Product in Air and Its Zinc Content

Copound	Percentage of zinc(II) oxide on thermal decomposition of reaction product in air		Percentage of zinc estimated (gravimetric method)	
	Found	Calcd	Found	Calcd
$Zn(OH)_2(8\text{-}HQ)_2$	20.46	20.88	16.52	16.77
$Zn(C_9H_6ON)_2$[a)]	20.84	23.01	18.26	18.48

a) Zinc oxinate prepared from solution.[11)]

Table 3. TG Data of Solid-State Reaction Product

Composition	Temp range	Wt loss/%		Loss of	Temp of oxide formation
		Obsd	Calcd		
	°C				°C
$Zn(OH)_2(8\text{-}HQ)_2$	—	—	—	—	—
$Zn(OH)_2(8\text{-}HQ)$	64.72—410	37.18	37.24	8-HQ	—
ZnO	410—753.63	39.38	41.86	8-HQ+H_2O	753.63

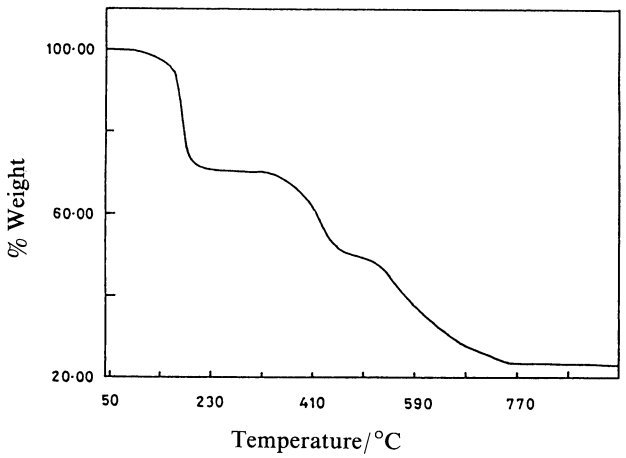

Fig. 2. TG curve for solid-state reaction product in nitrogen atmosphere.

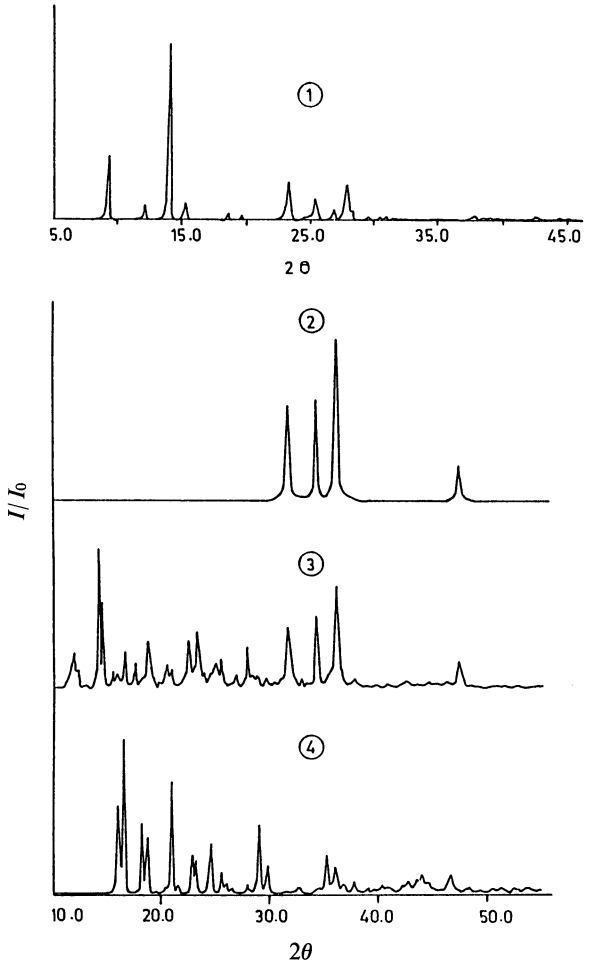

Fig. 3. Powder X-ray diffraction patterns of: 1. 8-HQ; 2. $Zn(OH)_2$; 3. Solid-state reaction product; 4. $Zn(C_9H_6ON)_2$ (prepared from solution).

$Zn(C_9H_6ON)_2$. The formation of $Zn(C_9H_6ON)_2$ as a subsidiary product has also been ruled out since none of its diffraction lines is observed in the diffraction pattern of reaction product. Therefore, the formation of reaction product in the solid state takes place according to chemical equation A and not B. Characterization of solid-state reaction product has also been done by IR spectral studies. There is a broad band observed between 3000—3300 cm^{-1} in the spectrum of solid 8-HQ. This band may be due to hydrogen bonded O–H group showing the dimeric structure of 8-HQ being stabilized by hydrogen bonding as reported by earlier worker.[12] A band at 1270 cm^{-1} in solid 8-HQ is due to (C–OH) group. This band is shifted to 1325 cm^{-1} in the spectrum of reaction product. Shifting of this band to higher frequency indicates that intermolecular hydrogen bonds in 8-HQ disappear on the formation of $Zn(OH)_2(8\text{-}HQ)_2$. Appearance of a band in the region 3620—3580 cm^{-1} is due to free O–H stretchings of 8-HQ in the reaction product. On the basis of these discussions the formation of solid-state reaction product may be visualized to take place as shown below.

Table 4. Interplanar Spacing (D) of Main Lines in the Powder X-Ray Diffraction Patterns

Compound	D Spacing / Å	I/I_0
$Zn(OH)_2$	2.4737	100.00
	2.6009	62.87
	2.8115	59.27
	1.4774	26.06
	1.6259	25.42
8-HQ	6.2650	100.00
	9.4739	35.19
	3.8163	22.08
	3.1880	21.34
	3.7878	13.62
$Zn(OH)_2(8\text{-}HQ)_2$	6.2507	100.00
	2.4781	69.53
	6.0997	63.61
	2.6068	49.13
	2.8189	42.98
$Zn(C_9H_6ON)_2$[a)]	5.3505	100.00
	4.2279	71.41
	5.5163	56.43
	4.8473	44.76
	3.0688	44.13

a) Prepared from solution.

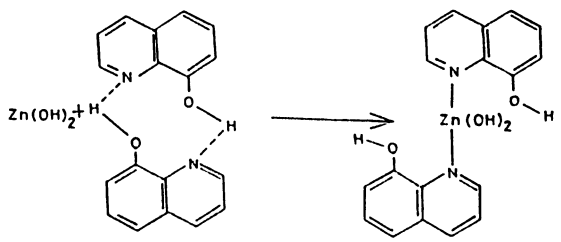

Now it is interesting to know as to how the reaction product is formed in the solid state. For this purpose the knowledge of crystal structure of zinc hydroxide and the

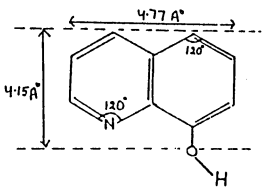

overall dimension of 8-HQ molecule as shown in the diagram, has been calculated by using the bond distance reported in the literature[12] with the assumption that CCC and CNC bond angles are ca. 120°. In calculating the overall dimensions of 8-HQ molecule the O–H bond distance has not been considered since hydrogen atom remains out of the plane of the ring for most of the conformations. The dimension of 8-HQ molecule is comparable with the interlayer space available in zinc hydroxide crystal which has layered structure similar to that of cadmium iodide. The interlayer space[13] in different forms of $Al(OH)_3$ are 4.72 Å (Bayerite), 4.79 Å (Nordstandete), and 4.85 Å (hydrargillite, monoclinic gibbsite). Assuming the interlayer space in $Zn(OH)_2$ crystal to be approximately of the same order as in different forms of $Al(OH)_3$, 8-HQ molecules can easily be accomodated in the interlayer space.

Intercalation of 8-HQ molecules may cause the interlayer space to increase and finally break leading to the formation of reaction product. Formation of intercalation compounds by species having layered structure is not very uncommon and has been reported in the literature.[14] Graphite forms large number of intercalation compounds with alkali metals, halogens, halide oxides, halides ($FeCl_3$, $AlCl_3$), and complex anions ($GaCl_4^-$, $AlCl_4^-$). In the formation of intercalation compounds an increase in the interlayer space has also been reported for WS_2 and MoS_2. The interlayer space in pure WS_2 (12.35 Å) is increased by 4.03, 4.84, and 5.53 Å by intercalation of K, Pb, and Cs respectively. It has also been reported that $Zn(OH)_2$ and $Cu(OH)_2$ should be able to intercalate flat organic molecules. Formation of zinc hydroxide nitrophenolates, zinc, cadmium, and copper hydroxide flavinates and inclusion complexes of Naphthol Yellow S with magnesium, copper, nickel, cobalt, mangane, and cadmium hydroxides have been reported. In these cases also the interlayer space has been reported to increase.

After establishing the stoichiometry of reaction product and its mode of formation, it is now useful to understand the mode of diffusion of 8-HQ through solid zinc hydroxide. For this purpose, kinetic studies in capillaries were carried out. When the reactants were kept in contact in capillaries, an yellow colored product was formed at the interface, with 8-HQ diffusing toward the hydroxide side. Thickness of the colored product increased at the product/zinc hydroxide interface which was measured at different time intervals. The data obeyed an empirical equation.

$$(\xi)^{n_1} = K_1 t, \qquad (1)$$

where ξ is the thickness of the product layer at any time t, K_1 is a constant related to the rate of reaction and n_1 is also a constant. It is to be stated that K_1 is not an absolute rate constant, instead it is an apparent rate constant and depends on the mode of diffusion of 8-HQ molecules through the product and the solid zinc hydroxide. The validity of Eq. 1 is established by the straight lines in $\log\xi$ vs. $\log t$ plots, Fig. 4, at different temperatures. Values of n_1 and K_1 were calculated from the slopes and intercepts of the straight lines (Fig.4) and shown in Table 5. Values of K_1 increase with increase of temperature according to an Arrhenius type equation

$$K_1 = A \exp(-E_a/RT), \qquad (2)$$

where E_a is the energy of activation, R is the gas constant, T is the absolute temperature, and A is a constant. Plot of $\log K_1$ values against $1/T$ gave a straight line, Fig. 5. From the slope of straight line the value of energy of activation (E_a) has been calculated to be 45.27 kJ mol^{-1}.

Increase in the length of the colored product layer observed under the microscope, is the measure of lateral

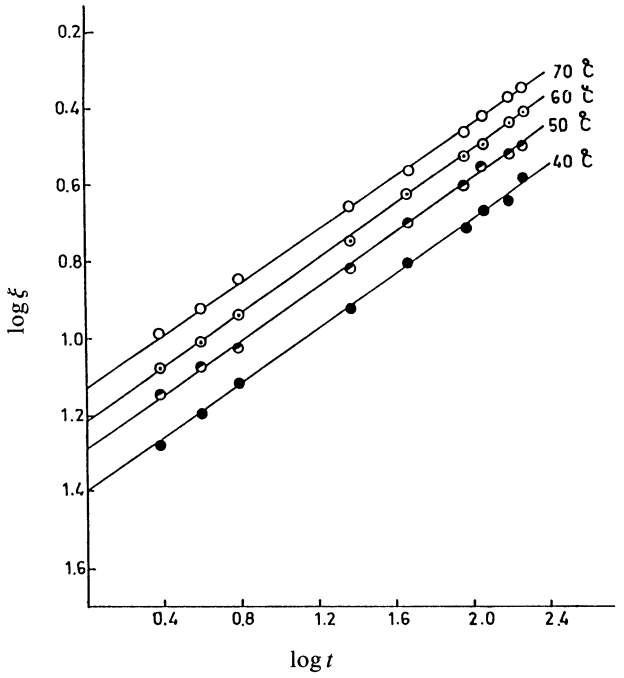

Fig. 4. Kinetic data for the reaction between $Zn(OH)_2$ and 8-HQ in contact at different temperatures.

Table 5. Value of K_1 and n_1 for the Reaction at Different Temperatures

Temperature ±1 °C	$K_1 \times 10^5$ / cm h^{-1}	n_1
40	9.3	2.88
50	18.2	2.90
60	28.8	2.88
70	49.0	2.93

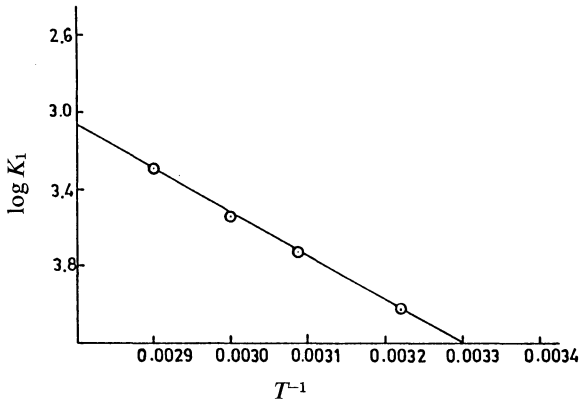

Fig. 5. Arrhenius plot showing the effect of temperature on the reaction rate, K_1.

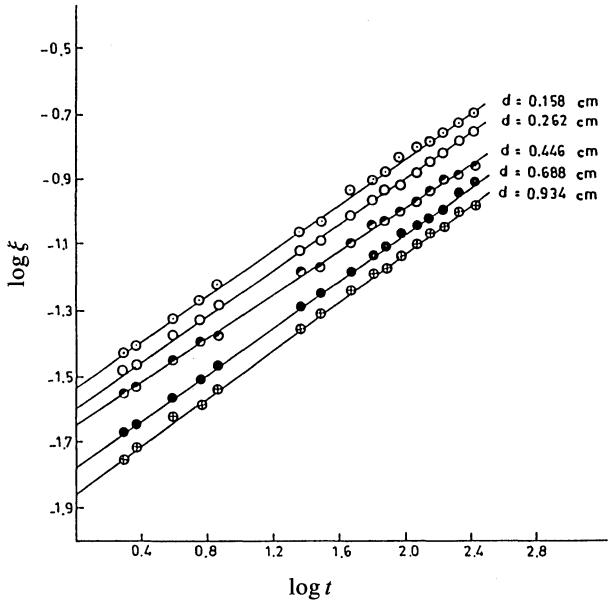

Fig. 6. Kinetic data with $Zn(OH)_2$ and 8-HQ, separated by air-gap at different lengths at 50±1 °C.

Table 6. Value of K_2 and n_2 When Reactants are Separated by Air-Gap of Different Lengths in Capillary at 50±1 °C

Length of air-gap between the reactants	$K_2 \times 10^5$	n_2
d (cm)	cm h^{-1}	
0.158	6.6	2.72
0.262	4.7	2.71
0.446	3.3	2.72
0.688	1.6	2.71
0.934	0.9	2.72

diffusion of 8-HQ molecules over the surface of solid zinc hydroxide. Therefore, the energy of activation, E_a is the activation energy for lateral diffusion of 8-HQ. Diffusion process may be expected to take place either by surface migration or vapor phase or by both the

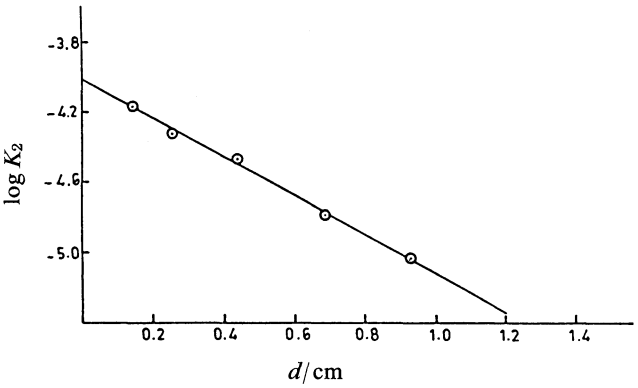

Fig. 7. Dependence of the rate constant, K_2, on the length of air-gap at 50±1 °C.

processes. In order to ascertain this contention kinetic studies in capillaries were performed by separating the reactants with air-gap of different lengths at 50±1 °C. The kinetic data satisfied Eq. 1 as shown in Fig. 6 with different magnitudes of constants (K_2 and n_2). The values of constants, K_2 and n_2, obtained from the straight lines shown in Fig. 6 are given in Table 6. The data given in Table 6 indicate that the value of K_2 decreases with increasing length of air-gap between the reactants. The variation in the value of his K_2 is in accordance with the following empirical relationship

$$K_2 = m \exp(-pd), \quad (3)$$

where m and p are constants and d is the length of the air-gap between the reactants. Plot of log K_2 values against d gives a straight line (Fig. 7). By extrapolating the straight line in Fig. 7 to d=0, a value of K_2 maybe obtained which should be equal to K_1 value (when the reactants were kept in contact) provided that the mecha-

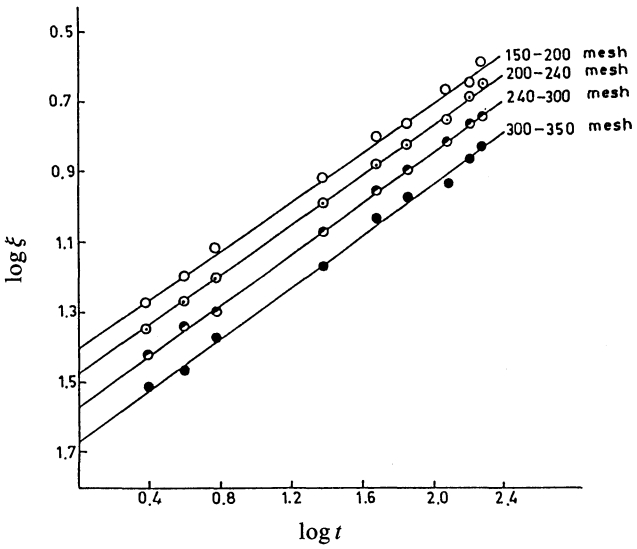

Fig. 8. Kinetic data for the reaction with reactants of different particle sizes (150—200 mesh, 200—240 mesh, 240—300 mesh, 300—350 mesh) at 40±1 °C.

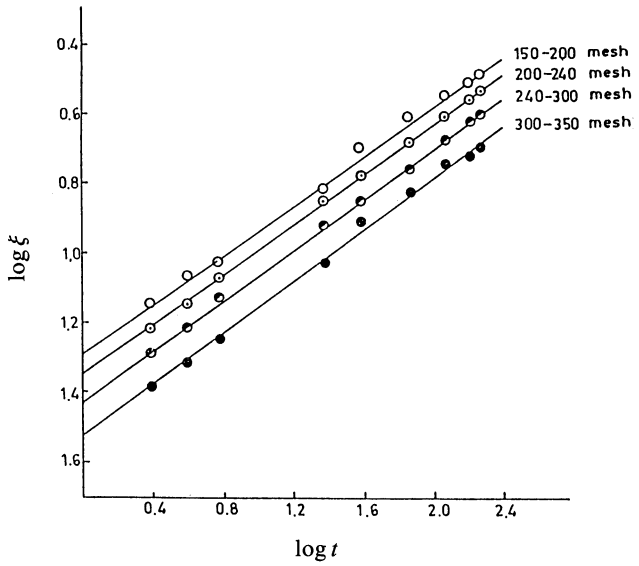

Fig. 9. Kinetic data for the reaction with reactants of different particle sizes (150—200 mesh, 200—240 mesh, 240—300 mesh, 300—350 mesh) at 50±1 °C.

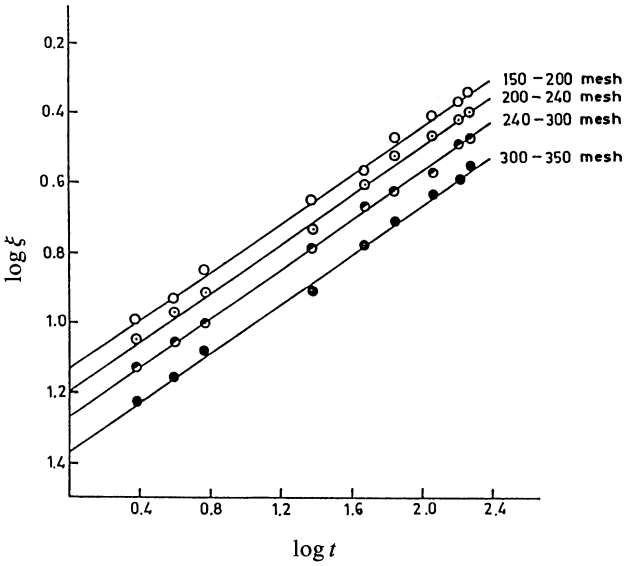

Fig. 11. Kinetic data for the reaction with reactants of different particle size (150—200 mesh, 200—240 mesh, 240—300 mesh, and 300—350 mesh) at 70±1 °C.

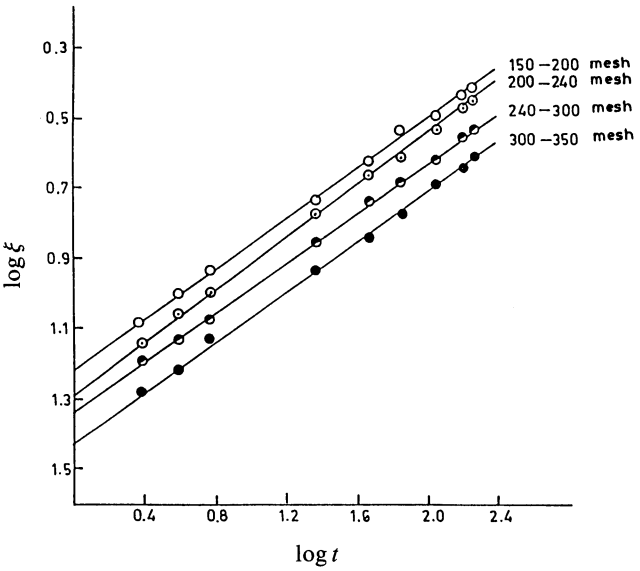

Fig. 10. Kinetic data for the reaction with reactants of different particle size (150—200 mesh, 200—240 mesh, 240—300 mesh, and 300—350 mesh) at 60± 1 °C.

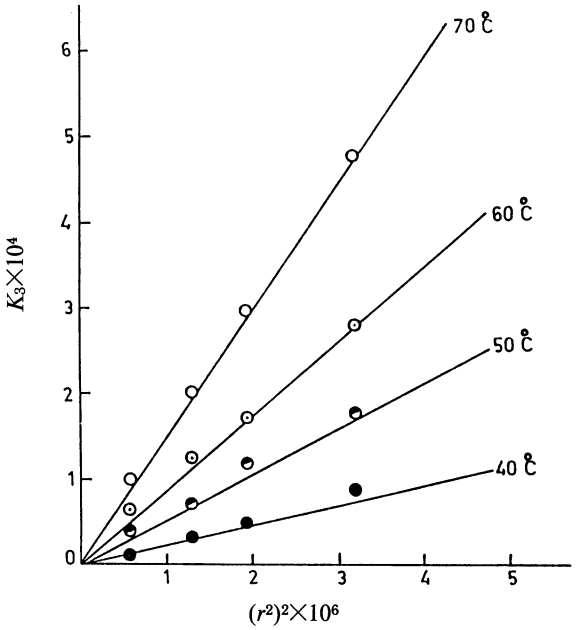

Fig. 12. K_3 vs. $(r^2)^2\times10^6$ plots showing the effect of particle size on rate constants.

nisms of diffusion involved in both the conditions were the same. The extrapolated K_2 value (9.1×10^{-5} cm h^{-1}) is significantly less than the K_1 value (18.20×10^{-5} cm h^{-1}) indicating the faster diffusion when reactants are kept in contact than when they are separated by air-gap. With reactants separated by air-gap, the diffusion is predominantly controlled by vapor phase. On the other hand, when they are kept in contact, surface migartion would also contribute significantly. Diffusion of 8-HQ by surface migration as well as by vapor phase has been established by other workers[15].

From the above discussions it is amply clear that surface migration plays a significant role during the diffusion of 8-HQ through solid zinc hydroxide. Surface migration of 8-HQ is likely to be affected by the particle size of the zinc hydroxide. In order to ascertain the role of particle size, kinetic studies with reactants of different particle sizes (200—240, 240—300, and 300—350 mesh nos.) have been performed. Kinetic data again obeyed the same empirical equation (1). Plots of $\log\xi$ vs. $\log t$ are shown in Figs. 8—11. In

Table 7. Value of K_3 and n_3 for Reactants of Different Particle Sizes at Different Temperatures

Temperature ±1 °C	Particle size (mesh no. of sieves)	$(r^2)^2\times10^6$	$K_3\times10^5$ / cm h^{-1}	n_3
40	150—200	3.27	9.3	2.88
	200—240	1.98	5.1	2.90
	240—300	1.36	3.8	2.88
	300—350	0.96	1.3	2.90
50	150—200	3.27	18.2	2.90
	200—240	1.98	12.3	2.90
	240—300	1.36	7.8	2.90
	300—350	0.96	4.3	2.90
60	150—200	3.27	28.8	2.88
	200—240	1.98	17.8	2.91
	240—300	1.36	13.2	2.90
	300—350	0.96	7.2	2.90
70	150—200	3.27	49.0	2.93
	200—240	1.98	30.9	2.93
	240—300	1.36	20.4	2.91
	300—350	0.96	10.1	2.92

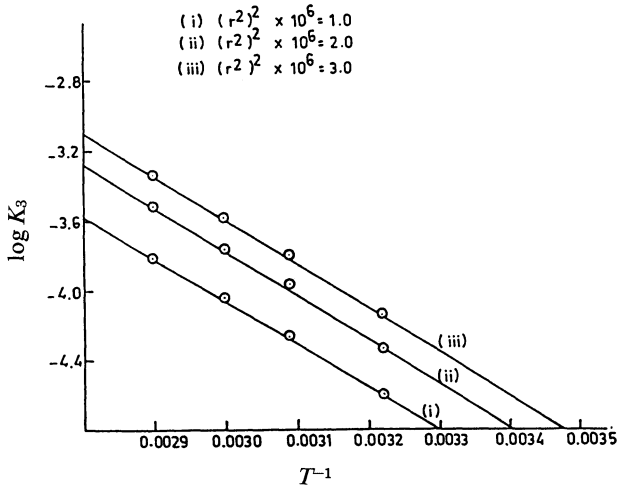

Fig. 13. Arrhenius plots showing the effect of temperature on reaction rate, K_3, for different $(r^2)^2\times10^6$ values.

these figures the data for particle size 150—200 mesh nos. are also shown for the purpose of comparison. From the straight lines in Figs. 8—11, the value of K_3 and n_3 were obtained. These values are shown in Table 7. Data given in Table 7 indicate that the value of K_3 depends on particle size. The larger the particle size, the greater the value of K_3 is. The variation in the value of K_3 with particle size is in accordance with the following empirical equation

$$K_3 = m(r^2)^2, \quad (4)$$

where m is a constant and r is the radii of the reactant (zinc hydroxide) particle. The value of r has been calculated from the mean values of the mesh nos. of the sieves with the assumption that the holes of the sieves are circular with radii r and the reactant particles passing through these holes are spherical with diameter $2r$. The plot of K_3 values against $(r^2)^2\times10^6$ values at different temperatures are shown in Fig. 12. From straight lines shown in Fig. 12 the values of K_3 for definite particle sizes ($(r^2)^2\times10^6$=1.0, 2.0, and 3.0) of the reactants have been calculated. The log K_3 vs. $1/T$ plots for each of these $(r^2)^2\times10^6$ values are shown in Fig. 13. From the slope of straight lines in Fig. 13, the magnitude of energy of activation has been calculated and given in Table 8. Data given in Table 8 indicate that the value of energy of activation does not depend on the particle size of the reactants although the value of rate constants depends on it (Table 7).

Table 8. Energy of Activation with Reactants of Different Particle Sizes

Particle size $(r^2)^2\times10^6$ / cm^4	Energy of activation / kJ mol^{-1}
1.0	45.53
2.0	45.37
3.0	45.41

The authors are thankful to Professor S. Giri, Head, Chemistry Department, Gorakhpur University for providing laboratory facilities. Thanks are also due to the authorities of RSIC, Nagpur for taking TG and powder X-ray diffraction pattern and CDRI, Lucknow for elemental analyses and IR spectral studies. Thanks are also due to CSIR, New Delhi for financial support.

References

1) N. B. Singh, R. P. Singh, and H. C. Singh, *J. Solid State Chem.*, **33**, 391 (1980).

2) M. A. Beg, A. Ahamad, and H. Askari, *J. Solid State Chem.*, **68**, 22 (1987).
3) P. S. Bassi, G. S. Chopra, and Kanwaljit Kaur, *Indian J. Chem., Sect. A*, **29**, 454 (1990).
4) A. F. Wells, "Structural Inorganic Chemistry," 4th ed, ELBS and Oxford University Press, Oxford (1979), pp. 516—558.
5) L. Mandelcorn, "Non-Stoichiometric Compounds," Academic Press, New York (1964), pp. 522—558.
6) R. P. Rastogi, P. S. Bassi, and S. L. Chaddha, *J. Phys. Chem.*, **67**, 2569 (1963).
7) R. P. Rastogi and B. L. Dubey, *J. Am. Chem. Soc.*, **89**, 200 (1967).
8) N. B. Singh and R. J. Singh, *J. Solid State Chem.*, **76**, 375 (1988).
9) "The Condensed Chemical Dictionary," 7th ed, Reinhold Publishing Corporation, New York (1966), p. 1034.
10) A. I. Vogel, "A Text Book of Quantitative Inorganic Analysis Including Elementary Instrumental Analysis," 3rd ed, The English Language Book Society and Longmans Green & Co., Ltd., Edinburgh (1962), pp. 532—533.
11) A. I. Vogel, "A Text Book of Quantitative Inorganic Analysis," 4th ed, ELBS and Longman, London (1978), pp. 422—423.
12) T. Banerjee and N. H. Saha, *Acta Crystallogr., Sect. C*, **42**, 1408 (1986).
13) A. F. Wells, "Structural Inorganic Chemistry," 4th ed, ELBS and Oxford University Press, Oxford (1979), pp. 523—525.
14) L. Mandelcorn, "Non-Stoichiometric Compounds," Academic Press, New York (1964), pp. 352—361.
15) R. P. Rastogi, N. B. Singh, and R. P. Singh, *J. Solid State Chem.*, **20**, 191 (1977).